Mn Oxide Nanoparticle Assemblies

Dynamic Organization of Inorganic Nanoparticles into Periodic Micrometer-Scale Patterns**

Oscar Giraldo, Jason P. Durand, Harikrishnan Ramanan, Kate Laubernds, Steven L. Suib, Michael Tsapatsis, Stephanie L. Brock, and Manuel Marquez*

Pattern formation, oscillations, and traveling fronts are widely found in nature.[1,2] Oscillatory phenomena in chemical and biochemical systems include carbon monoxide oxidation on single crystals of platinum,[3] seashell patterns,[4] aggregating slime molds,[5] banding textures in minerals,[6,7] and spiral waves in cardiac arrhythmias[8] and retinal tissue.[9] There has been an interest in the pattern formation of particles formed by self-assembly,[10–12] particularly those driven by physical factors, such as surface tension in evaporating colloidal solutions.[13–15] Herein, we present a study of oscillatory phenomena, in which inorganic nanoparticles are organized with a high degree of periodicity; these phenomena are exhibited in a similar fashion to Liesegang precipitation bands or rings,[16–18] or patterns of colloidal origin, which are formed in ionic or other precipitation–diffusion systems.

A simple synthesis of manganese oxide colloids has been developed.[19] Transmission electron microscopy (TEM) and small-angle neutron scattering (SANS) data show that the colloidal particles are of the order of 2–8 nm in diameter, with a disklike shape, and are dispersed in solution.[19] X-ray absorption spectroscopy indicates that the particles have a layered structure consisting of edge-shared MnO_6 octahedra; the Mn centers exhibiting an average oxidation state of 3.7.[20] These colloids can be organized[21–23] into structures and materials with multiscale ordering. Herein, the formation of inorganic films consisting of regular micrometer-sized parallel lines is reported. The composition and phase of the manganese oxide lines can be altered by ion-exchange or thermal treatment.

Micropatterns of mixed-valent manganese oxide colloids were self-assembled from dilute sols of tetramethylammonium (TMA) manganese oxide. A glass microscope slide was immersed vertically into a colloidal solution and was then placed into a preheated oven held at 85 °C until complete evaporation of the solvent had occurred (Figure 1a). The procedure results in a film composed of parallel lines (Figure 1b). Removal of the hydroxyl groups by silynation from the glass surface or using other types of hydrophobic

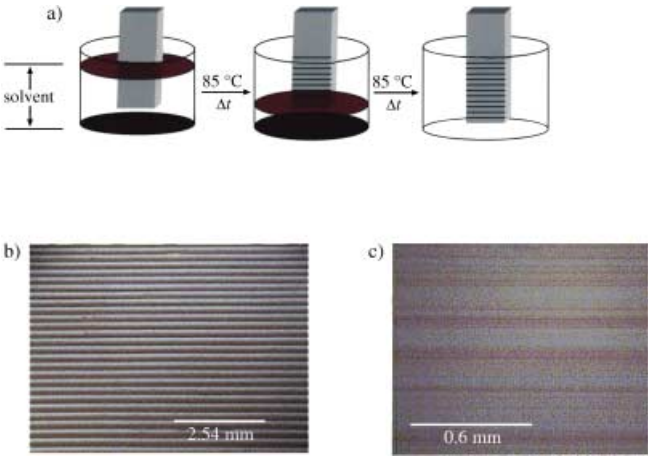

Figure 1. Tetramethylammonium manganese oxide sols form micropatterns of mixed-valent manganese oxide colloids. a) Schematic diagram of the pattern formation; b) self-assembled manganese oxide particles on a glass substrate composed of well-ordered parallel lines, obtained from hydrothermal treatment of a colloid solution; c) a continuous film found near the bottom of the substrate, which results from collapsed lines.

[*] Prof. S. L. Suib, J. P. Durand, K. Laubernds, S. L. Brock,[++] M. Marquez
Department of Chemistry, U-3060, University of Connecticut
55 North Eagleville Rd., Storrs, CT 06269-3060 (USA)
Fax: (+1) 860-486-2981
E-mail: suib@uconnvm.uconn.edu
O. Giraldo[+ ++]
Departamento de Química
Universidad Nacional de Colombia, Bogotá (Colombia)
H. Ramanan, M. Tsapatsis
Department of Chemical Engineering
159 Goessmann Laboratory, University of Massachusetts
Amherst, Massachusetts 01003-3110 (USA)
Prof. S. L. Suib
Department of Chemical Engineering, and Institute of Materials Science
University of Connecticut, Storrs, Connecticut 06269 (USA)
[+] Present address:
Departamento de Física y Química
Universidad Nacional de Colombia, Manizales (Colombia)
[++] Present address:
Department of Chemistry, Wayne State University
5101 Cass Avenue, Detroit, Michigan 48202

[**] We acknowledge Dr. Jim Romanow for helping to collect field emission electron microscopy data and the Institute of Materials Science at the University of Connecticut for use of the microscopy facilities for some of the TEM images. This work was made possible with the support of the Geosciences and Biosciences Division of the Office of Basic Energy Sciences, Office of Science, US Department of Energy.

 DOI: 10.1002/ange.200250712

surfaces, such as teflon, does not allow formation of patterns or any kind of film, which suggests that these patterns can only be assembled on hydrophilic surfaces. The measurements of average line width versus line number shows an increasing trend in the width of material deposition from top to bottom. Figure 2a shows the measurements of the line widths for films prepared with a molar Mn concentration of 10^{-3} M. All lines exhibit the trend seen in Figure 2a with the relative rate of the increase of width varying, until they collapse at the bottom part of the substrate forming a continuous film (Figure 1c). Figure 2c is a three-dimensional (3D) view of the intensity of the Mn signal obtained by X-ray fluorescence spectroscopy within a line (Figure 2b) that was produced from a 10^{-3} M colloidal TMA manganese oxide solution; the highest concentration of Mn appears to be near the center of the line.

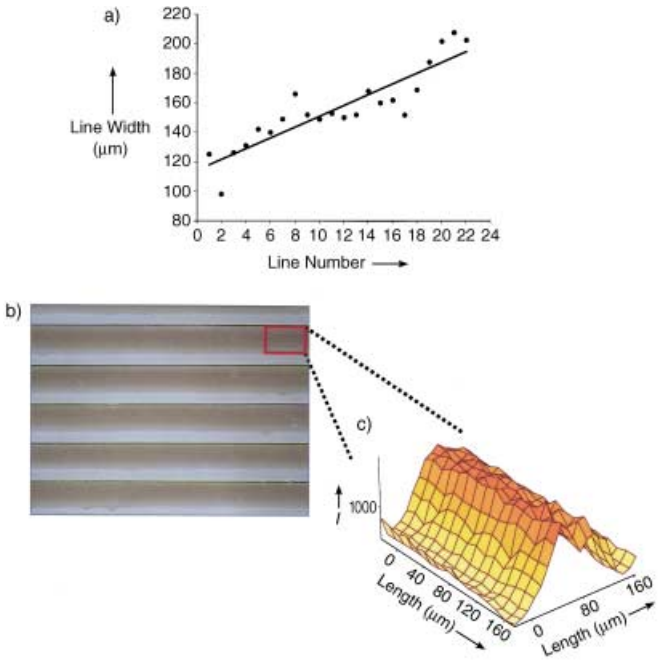

Figure 2. Methods of measuring lines deposited on to a substrate. a) The trend in line width observed in a specific sample while proceeding down the substrate; b) Mn X-ray fluorescence signal from the lines; c) 3D representation of the Mn X-ray fluorescence signal from a line.

Tapping-mode atomic force microscopy (TM-AFM) was used to measure the topography of the surface. Pronounced surface topography variations can be observed in the cross-sectional perspective (Figure 3a). Red arrows indicate height variations of 34.7 nm while the green ones indicate a variation of 14.7 nm. Surface topography variations are observed to run parallel to each other, which leads to the formation of lines, as shown in the 2D image (Figure 3b). Polarized optical microscopy shows that each line is formed of many thin lines, which are arranged in a stacked fashion (Figure 4a). The curved lines that are observed are caused by disturbances in the system during the formation processes that cause vibrations at the surface of the fluid. Figure 3c shows a 40 μm TM-AFM 3D image that illustrates the fine structure of the film. The film is composed of small agglomerations of material, with a broad particle-size distribution from several nanometers to micrometer size. Scanning electron microscopy (SEM) shows a film composed of agglomerations of material with particles of no defined morphology and a wide range of particle size (Figure 4b).

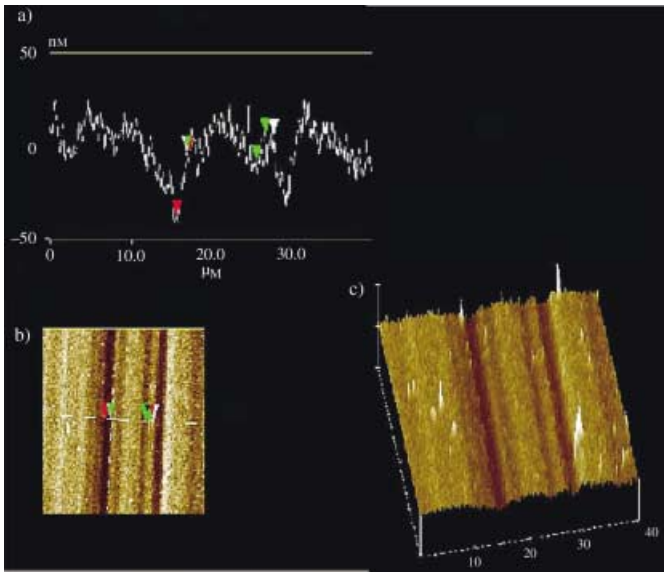

Figure 3. Tapping-mode atomic force microscopy data. a) Cross-sectional view of the surface topography over a 40 μm scan; b) 2D image of the topography, viewed from above the surface; c) 3D image of the 40 μm scan. I = intensity (counts s^{-1})

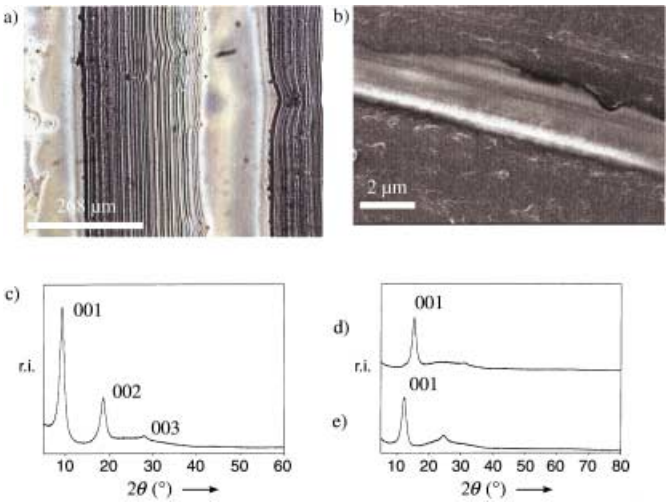

Figure 4. Structural and morphological studies of the manganese oxide micropatterns. a) Reflective optical micrograph indicating that each microline is comprised of many other smaller stacked lines; b) SEM image showing that the film is composed of an agglomeration of manganese oxide particles; c) XRD pattern showing the (00l) reflections of a layered phase, with the largest d spacing (9.8 Å (001)) corresponding to the interlayer separation; d) XRD pattern of a sample on which the lines had undergone ion-exchange with K^+ to remove TMA^+; e) XRD pattern of the same sample after calcination at 500 °C. r.i. = relative intensity.

X-ray diffraction (XRD) studies highlighted the occurrence of mesostructural order in the micropatterns (Figure 4c). Three evenly spaced reflections are observed which can be indexed to the (00*l*) reflections of a layered phase with the largest *d* spacing (0.98 nm; (001)) corresponding to the interlayer spacing. The XRD pattern is consistent with a structure composed of layers of edge-shared manganese oxide octahedra, analogous to the CdI_2 structure,[24] with the TMA cations between the MnO_x layers, without an effective hydration layer. XRD analysis of the deposit does not show the distinct (100) and (110) reflections that are expected.[25]

Complete removal of the organic cation (TMA^+) from the micropatterns can be achieved by ion-exchange using potassium, and leads to the formation of a layered phase corresponding to synthetic birnessite (OL-1) with an interlayer spacing of 0.72 nm (Figure 4d).[25] This phase features an effective hydration sheet with one metal cation residing between the manganese oxide layers. Calcination of the K-ion-exchanged micropatterns (K-OL-1) at 500 °C produced a new phase with an interlayer spacing of 0.57 nm (Figure 4e). This material corresponds to a dehydrated K-OL-1 phase that is also obtained with regular powdered materials under similar conditions.[26] The broad reflection between 15 and 40° (2θ) is an artifact from the glass slide.

TEM was used to examine the materials. Multiple analyses of the deposit shows that the layered material is mostly formed of large platelets (Figure 5a). A magnified view of the circled area in Figure 5a shows strands of a fiberlike structure that reveal the 1 nm layered spacing of the material (Figure 5b). As a result of the preferred orientation of the deposit, with layers assembled parallel to the glass slide (and therefore parallel to the TEM grid in the microtomed sample), the fiberlike structures are noticeable in very limited regions of the sample. The (001) spacing of 0.98 nm, determined by XRD, is in agreement with the 1 nm layered spacing observed by TEM imaging. The preferred orientation of the layers prevents the observation of the intralayer spacings by XRD. The electron diffraction (ED) pattern from the platelet shown in Figure 5c reveals the intralayer structure of the deposit (Figure 5d). The ED pattern is the [001] projection using an orthorhombic crystal geometry ($a = 1.04$, $b = 5.68$ nm). Based on both ED and XRD analysis, we determine that the crystal structure of the layered TMA manganese oxide has an orthorhombic unit cell.

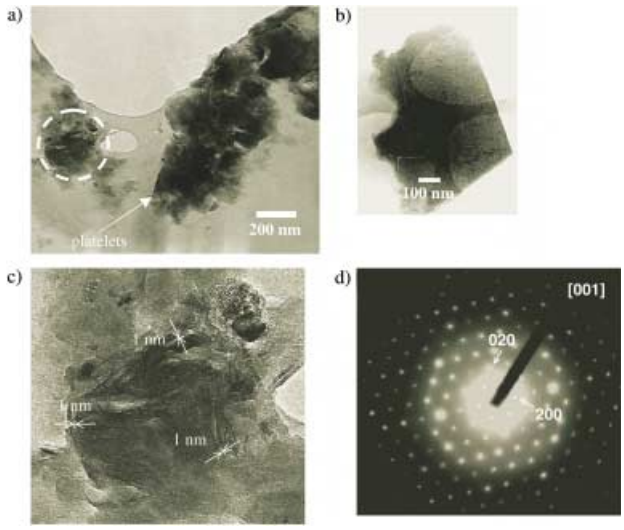

Figure 5. HR-TEM images of tetramethylammonium manganese oxide lines. a) Within the microscale line patterns, platelets are observed; b) a magnified image of the circular region in a), which shows strands and fibers observed with a 1 nm layered spacing; c) an individual platelet, which may correspond to the intralayer structure of the deposit; d) the electron diffraction pattern of the platelet c), indexed as the [001] projection using an orthorhombic crystal geometry ($a = 1.04$ nm, $b = 5.68$ nm).

Previous studies have confirmed the complex nature of the various crystal structures formed by layered manganese oxides.[27] Synthetic Na manganates exist as elongated platelets that give a pseudohexagonal symmetric ED pattern,[28] similar to that which is observed here. The wide range of unit cell dimensions deduced from the structural studies of various synthetic ion-exchanged layered manganese oxides confirms the flexibility of the framework structure.[27] Our TEM results are consistent with earlier studies of synthetic oxides that show ordered layers of MnO_6 octahedra with spacings of 0.96–1.01 nm.[29]

The assembly of the inorganic nanoparticles on a hydrophilic substrate to form well-organized micrometer-scale patterns depends on factors such as surface tension, convection, crystal growth, and particle–particle and particle–substrate interactions. The colloidal solution wets the substrate in a capillary-rise geometry to which the contact line (air/fluid/substrate interface) climbs out of the reservoir forming a meniscus. Since the assembly is carried out at 85 °C, there is a continuous evaporation of the solvent[24,19] at the surface of the fluid, as well as convection from the bottom to the top.

The primary particles (2–8 nm in diameter) start to grow in the bulk of the solution as a consequence of the temperature, and have been observed by SANS data and UV/Vis spectroscopy.[19] Figure 6 shows that the particles initially agglomerate into clusters and these form larger particles that have an elliptical shape. These particles grow by an Ostwald ripening mechanism,[30] in which the growth of the large particles occurs at the expense of the smaller ones. Finally, the elliptical particles associate to form large platelike particles (Figure 6b).

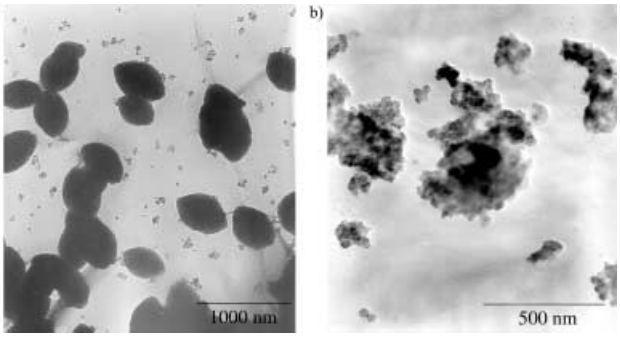

Figure 6. TEM images of a tetramethylammonium manganese oxide colloidal solution. a) Particles agglomerating into clusters; b) larger particles formed over time exhibit an elliptical shape.

As particle growth proceeds, the particles move, driven by convection, and when they reach the surface of the fluid they rapidly propagate in a horizontal mode driven by the Marangoni effect,[31] which is a surface-tension driven convection effect induced by a temperature gradient and evaporation. When the nanoparticles reach the contact line, they interact strongly with the substrate and precipitate. Large particles will interact more with the substrate and will induce the adhesion of more material. The fact that assembly only occurs at a hydrophilic surface indicates that the substrate–particle interaction may result from hydrogen bonding through hydroxy groups.

The concentration of nanoparticles in the meniscus should be greater than in the bulk,[32] which will result in a faster crystal growth at the drying line, with respect to the bulk. The periodicity that is observed is directly related to variations in the concentration of the large nanoparticles in the meniscus that are continuously fed with the nanoparticles that diffuse from the bulk. As the solvent evaporates there is less fluid left, so that the distance through which the particles have to diffuse is shorter, and the feeding rate at the meniscus increases, which results in greater deposition of material at the substrate. This is experimentally observed as an increase in the line width. The periodic precipitation phenomena might have a close analogy with Liesegang rings, however they are distinct in that precipitation takes place at a drying front rather than in a gel.[33]

These results demonstrate that as a result of time, interaction with a glass surface, surface tension, and crystal growth, these nanoparticles undergo self-assembly from a dissociated colloid. An ordered microarray of lines is composed of nanoparticles that have increased in size relative to those in the original solution and which have a layered structure. These lamellar inorganic micropatterns can undergo ion-exchange reactions with retention of the layered structure. New generations of materials with wide ranges of composition could be readily prepared by ion-exchange methods. These materials can be thermally modified to produce other phases, and therefore may provide templates for a variety of applications. The unique features of these systems include the unusual periodicity, morphology, simple preparation, ease of ion-exchange, and transformations to alternate structures, while preserving the morphology.

Experimental Section

A colloidal solution of lamellar manganese oxide (0.1 M, with respect to Mn) was prepared by adding $((CH_3)_4N)MnO_4$ (10 mmol) to a stirred mixture of distilled deionized water (100 mL) and 2-butanol (30 mL) at room temperature. After 30 min, a dark red-brown solution was formed in the lower aqueous layer. This aqueous solution was isolated from the upper organic layer with a separating funnel and then either used as obtained, or diluted (to 10^{-3} M, with respect to Mn).

The Advanced Photon Source at Argonne National Laboratories was used to study the manganese concentration in $(TMA)_yMnO_x$ lines. TM-AFM images were collected with a NanoScope MultiMode scanning probe microscope (Nanoscope III system controller) from Digital Instruments. Optical microscopy data were obtained on a Kramer video microscopy system with a JVC CCD color video camera.

The $(TMA)_yMnO_x$ lines were ion-exchanged with K^+ ions for preparation of synthetic birnessite (K-OL-1). The ion-exchange reaction was carried out at room temperature by immersing the films in an aqueous solution of KNO_3 (0.1 M), followed by an extensive washing step with deionized water. Finally, the samples were dried in air at room temperature.

High-resolution transmission electron microscopy (HR-TEM) studies of the TMA–manganese oxide lines on glass slides were carried out using a JEOL 3010 microscope operated at 300 kV. Samples of the lines were prepared by transferring small amounts of the deposit from the slides into curing molds and pouring a few drops of epoxy resin over them. To ensure the curing was hard enough for microtoming, the samples were allowed to cure for 3–5 h at 45 °C. The surface was then microtomed (at room temperature conditions, 25 °C) to obtain thin sections on sample grids (Carbon holey film grids, Ted Pella, Inc.) for TEM analysis. Some samples were also prepared from dilute suspensions of the crushed deposit in deionized water. Similar observations were obtained from samples prepared by either of the methods. For TEM analysis of the colloidal suspension, the solution was dropped onto a holey carbon 300 mesh copper grid (SPI). HR-SEM was performed on a Zeiss DSM 982 Gemini field-emission scanning electron microscope.

Received: December 6, 2002
Revised: April 8, 2003 [Z50712]

Keywords: colloids · manganese · nanomaterials · oxides · self-assembly

[1] S. Scott, *Oscillations, Waves and Chaos in Chemical Kinetics*, Oxford Universtiy Press, Oxford, **1995**.
[2] P. Ball, *The Self-Made Tapestry: Pattern Formation in Nature*, Oxford Universtiy Press, Oxford, **1999**.
[3] S. Jakubith, H. H. Rotermund, W. Engel, A. von Oertzen, G. Ertl, *Phys. Rev. Lett.* **1990**, *65*, 3013.
[4] H. Meinhardt, *The Algorithmic Beauty of Sea Shells*, Springer, Berlin, **1995**.
[5] F. Siegert, C. J. Weijer, *Cell Sci.* **1989**, *93*, 325.
[6] R. F. Cooper, J. B. Fanselow, J. K. R. Weber, D. R. Merkley, D. B. Poker, *Science* **1996**, *274*, 1173.
[7] C. Frondel, *Am. Mineral.* **1978**, *63*, 17.
[8] J. M. Davidenko, A. V. Pertsov, R. Salomonsz, W. Baxter, J. Jalife, *Nature* **1992**, *355*, 349.
[9] N. L. Gorelova, J. Bures, *J. Neurobiol.* **1983**, *14*, 353.
[10] A. N. Shipway, E. Katz, I. Willner, *ChemPhysChem* **2000**, *1*, 18.
[11] Y. Xia, J. A. Rogers, K. E. Paul, G. M. Whitesides, *Chem. Rev.* **1999**, *99*, 1823.
[12] H. H. Wickman, J. N. Korley, *Nature* **1998**, *393*, 445.
[13] P. C. Ohara, J. R. Heath, W. M. Gelbart, *Angew. Chem.* **1997**, *109*, 1120; *Angew. Chem. Int. Ed. Engl.* **1997**, *36*, 1078.
[14] M. Maillard, L. Motte, A. T. Ngo, M. P. Pileni, *J. Phys. Chem. B* **2000**, *104*, 11871.
[15] H. Wang, Z. Wang, L. Huang, A. Mitra, Y. Yan, *Langmuir* **2001**, *17*, 2572.
[16] H. K. Henisch, *Crystals in Gels and Liesegang Rings*, Cambridge Universtiy Press, New York, **1988**.
[17] K. F. Mueller, *Science* **1984**, *225*, 1021.
[18] M. Tsapatsis, D. G. Vlachos, S. Kim, H. Ramanan, G. R. Gavalas, *J. Am. Chem. Soc.* **2000**, *122*, 12864.
[19] S. L. Brock, M. Sanabria, S. L. Suib, V. Urban, P. Thijyagarajan, D. Potter, *J. Phys. Chem. B* **1999**, *103*, 7416.
[20] T. Ressler, S. L. Brock, J. Wong, S. L. Suib, *J. Phys. Chem. B* **1999**, *103*, 6407.
[21] O. Giraldo, S. L. Brock, M. Marquez, S. L. Suib, H. Hillhouse, M. Tsapatsis, *Nature* **2000**, *405*, 38.

[22] O. Giraldo, S. L. Brock, M. Marquez, S. L. Suib, H. Hillhouse, M. Tsapatsis, *J. Am. Chem. Soc.* **2000**, *122*, 12158.
[23] M. Marquez, J. Robinson, V. Van Nostrand, D. Schaefer, L. Ryzhkov, W. Lowe, S. L. Suib, *Chem. Mater.* **2002**, *14*, 1493.
[24] E. Silvester, A. Manceau, V. A. Drits, *Am. Mineral.* **1997**, *82*, 962 – 978.
[25] R. N. DeGuzman, Y. F. Shen, S. L. Suib, B. R. Shaw, C. L. O'Young, *Chem. Mater.* **1993**, *5*, 1395.
[26] J. Luo, Q. Zhang, A. Huang, O. Giraldo, S. L. Suib, *Inorg. Chem.* **1999**, *38*, 6106.
[27] K. Kuma, A. Usui, W. Paplawsky, B. Gedulin, G. Arrhenius, *Mineral. Mag.* **1994**, *58*, 425.
[28] R. Giovanoli, E. Stahli, W. Feitknecht, *Helv. Chim. Acta* **1970**, *53*, 209.
[29] R. Giovanoli, in *Geology and Geochemistry of Manganese, Vol. 1* (Eds.: I. M. Varentsov, G. Grasselly), Akad. Kiado, Budapest, **1980**, pp. 159 – 202.
[30] A. Baldan, *J. Mater. Sci.* **2002**, *37*, 2171.
[31] X. Fanton, A. M. Cazabat, *Langmuir* **1998**, *14*, 2554.
[32] Y. Lu, R. Ganguli, C. A. Drewien, M. T. Anderson, C. J. Brinker, W. Gong, Y. Guo, H. Soyez, B. Dunn, M. H. Huang, J. I. Zink, *Nature* **1997**, *389*, 365.
[33] R. E. Liesegang, *Naturwissenschaften* **1896**, *11*, 353.

